The kinetically dominant assembly pathway for centrosomal asters in *Caenorhabditis elegans* is γ-tubulin dependent

Eva Hannak,[1] Karen Oegema,[1] Matthew Kirkham,[1] Pierre Gönczy,[2] Bianca Habermann,[1] and Anthony A. Hyman[1]

[1]Max Planck Institute of Molecular Cell Biology and Genetics, 01307 Dresden, Germany
[2]Institut Suisse de Recherche Expérimentale sur le Cancer, CH-1066 Epalinges s/Lausanne, Switzerland

γ-Tubulin–containing complexes are thought to nucleate and anchor centrosomal microtubules (MTs). Surprisingly, a recent study (Strome, S., J. Powers, M. Dunn, K. Reese, C.J. Malone, J. White, G. Seydoux, and W. Saxton. *Mol. Biol. Cell.* 12:1751–1764) showed that centrosomal asters form in *Caenorhabditis elegans* embryos depleted of γ-tubulin by RNA-mediated interference (RNAi). Here, we investigate the nucleation and organization of centrosomal MT asters in *C. elegans* embryos severely compromised for γ-tubulin function. We characterize embryos depleted of ~98% centrosomal γ-tubulin by RNAi, embryos expressing a mutant form of γ-tubulin, and embryos depleted of a γ-tubulin–associated protein, CeGrip-1. In all cases, centrosomal asters fail to form during interphase but assemble as embryos enter mitosis. The formation of these mitotic asters does not require ZYG-9, a centrosomal MT-associated protein, or cytoplasmic dynein, a minus end–directed motor that contributes to self-organization of mitotic asters in other organisms. By kinetically monitoring MT regrowth from cold-treated mitotic centrosomes in vivo, we show that centrosomal nucleating activity is severely compromised by γ-tubulin depletion. Thus, although unknown mechanisms can support partial assembly of mitotic centrosomal asters, γ-tubulin is the kinetically dominant centrosomal MT nucleator.

Introduction

Proper regulation of the microtubule (MT)* cytoskeleton is required to organize the interphase cytoplasm and assemble a spindle during mitosis. The cell controls the organization of the MT cytoskeleton in part by accelerating the rate of MT nucleation in a spatially defined way. This is possible because there is a kinetic barrier that makes initiation of new polymers less favorable than elongation of existing ones (Alberts et al., 1994). Centrosomes, the major MT organizing centers in animal cells, play a central role in MT nucleation (for reviews see Kellogg et al., 1994; Tassin and

Bornens, 1999). Centrosomes consist of a pair of centrioles surrounded by an electron dense matrix called the pericentriolar material (PCM). In animal cells, when MTs are depolymerized by cold or treatment with drugs and then allowed to repolymerize by rewarming or removal of drugs, MT regrowth selectively initiates from the PCM (Frankel, 1976; Osborn and Weber, 1976; Keryer et al., 1984; Meads and Schroer, 1995), demonstrating the ability of the centrosome to accelerate MT nucleation in vivo.

Our understanding of how centrosomes promote MT nucleation is derived largely from studies of γ-tubulin, a specialized tubulin that localizes to centrosomes and is conserved among eukaryotes. Genetic studies have demonstrated that γ-tubulin has a role in MT assembly in *Aspergillus nidulans*, *Schizosaccharomyces pombe*, *Drosophila melanogaster*, and *Saccharomyces cerevisiae* (for reviews see Pereira and Schiebel, 1997; Oakley, 2000). Injection of antibodies to γ-tubulin into vertebrate tissue culture cells inhibits the regrowth of interphase MT arrays after depolymerization and prevents the assembly of a functional spindle during mitosis (Joshi et al., 1992). Assembly of

Figure 1. **The assembly of centrosomal asters in *tbg-1(RNAi)* embryos correlates with the presence of visibly condensed DNA.** Embryos were fixed and stained for MTs (left), γ-tubulin (middle), and DNA (right). All panels are aligned with anterior to the left and posterior to the right. (A) During interphase, before visible DNA condensation, MTs grow from the still unseparated centrosomes in wild-type embryos (top, white arrows). Numerous cytoplasmic MTs are also present. In *tbg-1(RNAi)* embryos (bottom), cytoplasmic MTs are not affected but no centrosomal asters are detected. Remnants of the spindle from the second meiotic division of the oocyte pronucleus are visible in the anterior of both embryos (black arrows). (B) During mitotic prophase, the centrosomal asters in wild-type embryos have increased in size and are located between the two pronuclei (top, white arrows). In *tbg-1(RNAi)* embryos, MT asters form around unseparated centrosomes (bottom, arrow) positioned behind the sperm pronucleus. (C) After NEBD, a bipolar spindle is assembled in wild-type embryos (top). In *tbg-1(RNAi)* embryos, centrosomal asters have increased in size, but a mitotic spindle does not assemble (bottom). The DNA from the oocyte and sperm pronuclei remains in separate masses and does not align on a metaphase plate. Note that in some cases, our γ-tubulin antibody weakly stains condensed chromosomes (C, top middle). This staining does not disappear in *tbg-1(RNAi)* embryos (B, bottom middle). Bar, 10 μm.
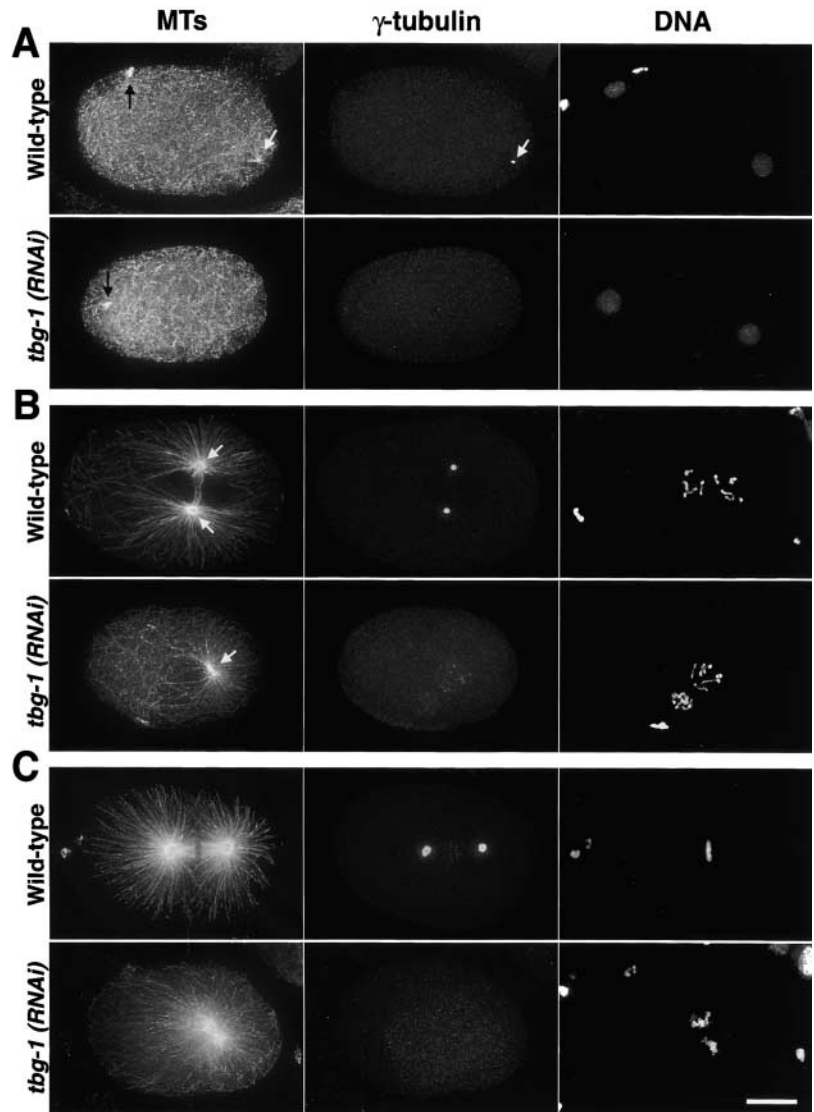
sperm centrosomal asters is also impaired when γ-tubulin function is inhibited in *Xenopus* egg extracts (Felix et al., 1994; Stearns and Kirschner, 1994).

γ-Tubulin functions in the context of larger protein complexes (for reviews see Jeng and Stearns, 1999; Wiese and Zheng, 1999; Schiebel, 2000). In all eukaryotes where it has been examined, γ-tubulin is in a heteromeric complex with two members of the Spc97p/Spc98p family of proteins. In higher eukaryotes, this "small" complex (γ-TuSC) is a subunit of a larger structure called the γ-tubulin ring complex (γ-TuRC; Zheng et al., 1995; Oegema et al., 1999). The γ-TuRC has a lock washer–like structure (Zheng et al., 1995; Moritz et al., 2000) approximately the diameter of an MT (25 nm). Isolated γ-TuRCs can nucleate and cap MTs in vitro (Zheng et al., 1995; Oegema et al., 1999; Wiese and Zheng, 2000). Elegant structural studies have shaped our ideas of how the γ-TuRC functions in the context of the PCM. Rings that have the same diameter as the γ-TuRC have been visualized by EM tomography in the PCM of centrosomes isolated from *Drosophila* (Moritz et al., 1995a) and *Spisula* (Vogel et al., 1997). In *Drosophila*, immunoelectron microscopy confirmed the presence of clusters of γ-tubulin

in the ring structures and at the base of the MTs polymerized off centrosomes in vitro (Moritz et al., 1995b). Cumulatively, these results suggest that γ-tubulin–containing complexes nucleate MTs both in vitro and in vivo.

A role for the γ-TuRC in anchoring of centrosomal MTs is also possible. Centrosomes extracted with potassium iodide reveal a structural network of 12–15-nm fibers termed the "centromatrix" (Schnackenberg et al., 1998). The centromatrix lacks 25-nm ring structures and has no nucleating activity of its own. When incubated with embryo extract or γ-tubulin–containing fractions, the centromatrix recovers nucleating activity and ring structures are again observed in samples examined by EM tomography (Moritz et al., 1998; Schnackenberg et al., 1998). These studies have led to the model that the centromatrix anchors the γ-TuRC in a relatively direct fashion through the help of an adaptor molecule (Moritz et al., 1998). If MTs remain attached to the γ-TuRC after nucleation, this connection would indirectly tether MTs to the centromatrix.

Despite the body of information suggesting a central role for γ-tubulin in centrosomal MT nucleation, Sampaio et al. (2001) have recently shown that organized cen-

trosomal asters assemble during prophase in *Drosophila* spermatocytes severely depleted of γ-tubulin. Strome et al. (2001) have also shown that prominent mitotic asters form in *Caenorhabditis elegans* embryos depleted of γ-tubulin by RNA-mediated interference (RNAi). Here we use a combination of RNAi and genetic approaches to investigate the mechanisms that nucleate and organize centrosomal MT asters in *C. elegans* embryos severely compromised for γ-tubulin function. We show that although assembly of centrosomal asters fails during interphase in these embryos, unknown mechanisms can support partial assembly of mitotic centrosomal asters. However, even in mitotic embryos, centrosomal nucleating activity is severely compromised by γ-tubulin depletion, suggesting that γ-tubulin is the kinetically dominant centrosomal MT nucleator.

Results

Centrosomal asters fail to form during interphase in *tbg-1(RNAi)* embryos, but assemble as embryos enter mitosis

The *C. elegans* genome sequencing project identified one gene homologous to γ-tubulin, *tbg-1*. Strome et al. (2001) recently reported that robust MT asters were present in mitotic embryos depleted of γ-tubulin by RNAi (hereafter referred to as *tbg-1[RNAi]* embryos). We began our study by characterizing the cell cycle–dependent organization of the MT cytoskeleton in *tbg-1(RNAi)* embryos to determine when during the cell cycle centrosomal asters assemble. We fixed wild-type and *tbg-1(RNAi)* embryos and stained them to visualize MTs, γ-tubulin, and DNA. Three-dimensional (3D) wide field images were collected and deconvolved; projections of the 3D stacks are shown (Fig. 1). During *C. elegans* fertilization, the sperm brings a centriole pair into the egg (which lacks centrioles) together with the sperm pronucleus. This centriole pair duplicates and recruits PCM components, including γ-tubulin, from the cytoplasm, resulting in two centrosomes sitting side by side that are associated with the sperm pronucleus (Fig. 1 A, top). The centrosomes separate and the oocyte-derived pronucleus migrates toward the sperm pronucleus. The pronuclei meet (Fig. 1 B, top), the nuclear envelope breaks down, and a spindle assembles with two prominent foci of γ-tubulin, corresponding to the spindle poles, on either side of the metaphase plate (Fig. 1 C, top). In contrast to wild type, γ-tubulin was essentially absent from centrosomes in *tbg-1(RNAi)* embryos (Fig. 1, A–C, bottom), confirming depletion by RNAi (see quantification of depletion below).

The effect of γ-tubulin depletion on the MT network was dramatic (Fig. 1, A–C, left). Prior to mitotic prophase, wild-type embryos were filled with cytoplasmic MTs, and astral MTs emanated from the two centrosomes associated with the sperm-derived pronucleus in the posterior of the embryo (Fig. 1 A, top left). In contrast, in *tbg-1(RNAi)* embryos, although the cytoplasmic MTs appeared unaffected, astral MTs were absent before the initiation of visible DNA condensation (Fig. 1 A, bottom left). Interestingly, *tbg-1(RNAi)* embryos that contained nuclei with visibly condensed chromosomes were able to organize centrosomal asters (Fig. 1 B, bottom left). After nuclear envelope breakdown (NEBD), centrosomal asters
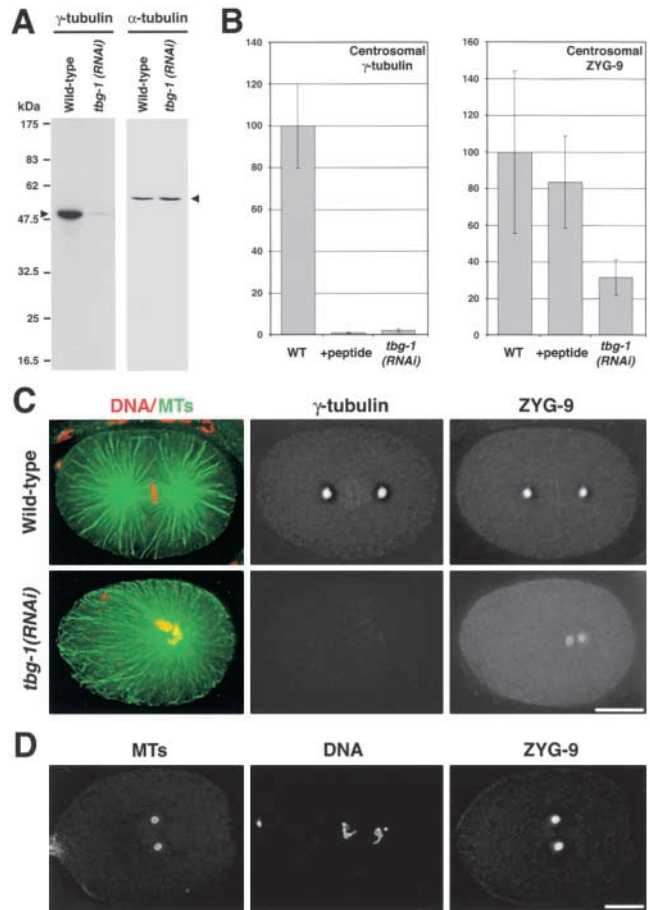
Figure 2. **Quantification of γ-tubulin depletion and reduction of centrosomal ZYG-9 in *tbg-1(RNAi)* embryos.** (A) A Western blot of wild-type (left lanes) and *tbg-1(RNAi)* (right lanes) embryos was probed with antibodies to γ-tubulin (left panel) and α-tubulin (right panel). Bands corresponding to γ- and α-tubulin are indicated (arrowheads). (B) Quantification of centrosomal γ-tubulin and ZYG-9 fluorescence in wild-type (WT) and *tbg-1(RNAi)* embryos. Centrosomes in eight embryos were quantified for each condition. Total centrosomal fluorescence is expressed in arbitrary units. Error bars are the standard deviation. (C) Sample images from the embryos quantified in B. Wild-type (top) and *tbg-1(RNAi)* embryos (bottom) were fixed and stained for MTs and DNA (left), γ-tubulin (middle), and ZYG-9 (right). (D) A nocodazole-treated embryo fixed and stained for MTs (left), DNA (middle), and ZYG-9 (right). Bars, 10 μm.

in both wild-type (Fig. 1 C, top left) and *tbg-1(RNAi)* embryos (Fig. 1 C, bottom left) increased in size. Despite the formation of prominent mitotic centrosomal asters, spindle assembly always failed in *tbg-1(RNAi)* embryos. These results suggest that during interphase, γ-tubulin is required to assemble centrosomal asters, but not to nucleate or stabilize cytoplasmic MTs. Upon mitotic entry, *tbg-1(RNAi)* embryos gain the ability to assemble centrosomal asters.

Centrosomal γ-tubulin is reduced by ~98% in *tbg-1(RNAi)* embryos

The assembly of mitotic centrosomal asters in *tbg-1(RNAi)* embryos suggests that γ-tubulin–independent mechanisms might contribute to the nucleation and organization of centrosomal asters. However, to make this conclusion, it is important to quantify the extent of the γ-tubulin depletion.

Figure 3. ***tbg-1(t1465)* mutants have a mutation in a residue highly conserved among tubulins.** (A) *tbg-1(t1465)* is a point mutation that leads to the substitution of alanine 401 with valine. A sequence alignment of the COOH termini of α-, β-, and γ-tubulins from *S. cerevisiae* and *C. elegans,* α- and β-tubulin from pig, and human γ-tubulin from human is shown. Amino acids cons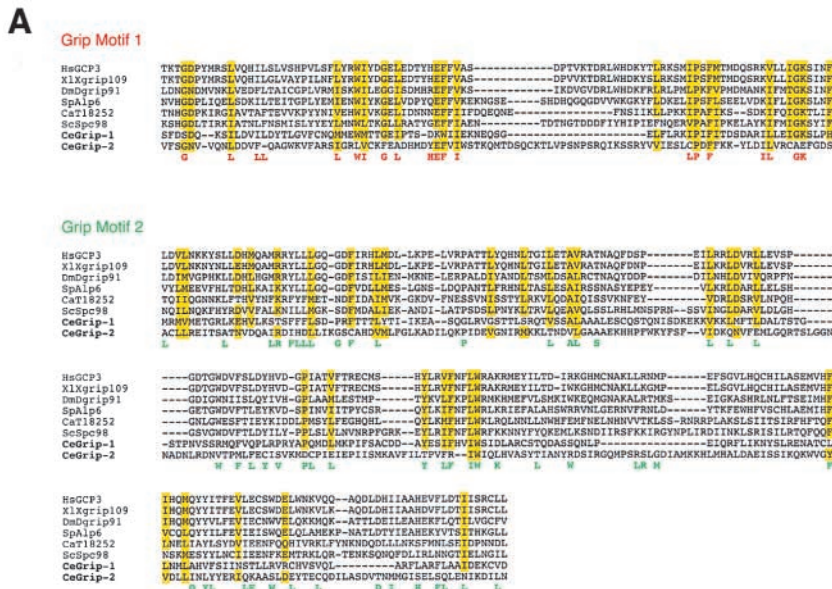erved in 80–100% of the sequences are highlighted in yellow and alanine 401 is in red. Arrows and tubes above the alignment indicate conserved β sheets and α helices, respectively (Nogales et al., 1998). (B–D) Characterization of the MT cytoskeleton in *tbg-1(t1465)* embryos. (B) An interphase *tbg-1(t1465)* embryo stained for MTs (left) and DNA and γ-tubulin (blue and red, right). A remnant of the spindle from the second meiotic division of the oocyte pronucleus is visible (black arrow), but no centrosomal asters are detected. γ-Tubulin localizes to centrosomes (arrows) that fail to associate with the sperm pronucleus (arrowhead). (C) Mitotic *tbg-1(t1465)* embryos were stained for MTs (left), γ-tubulin (middle), and DNA (right). Two typical examples are shown here (top and bottom). (D) Mitotic *tbg-1(t1465+RNAi)* embryos stained for MTs and ZYG-9 (green and red, left), γ-tubulin (middle), and DNA (right). Bar, 10 μm.
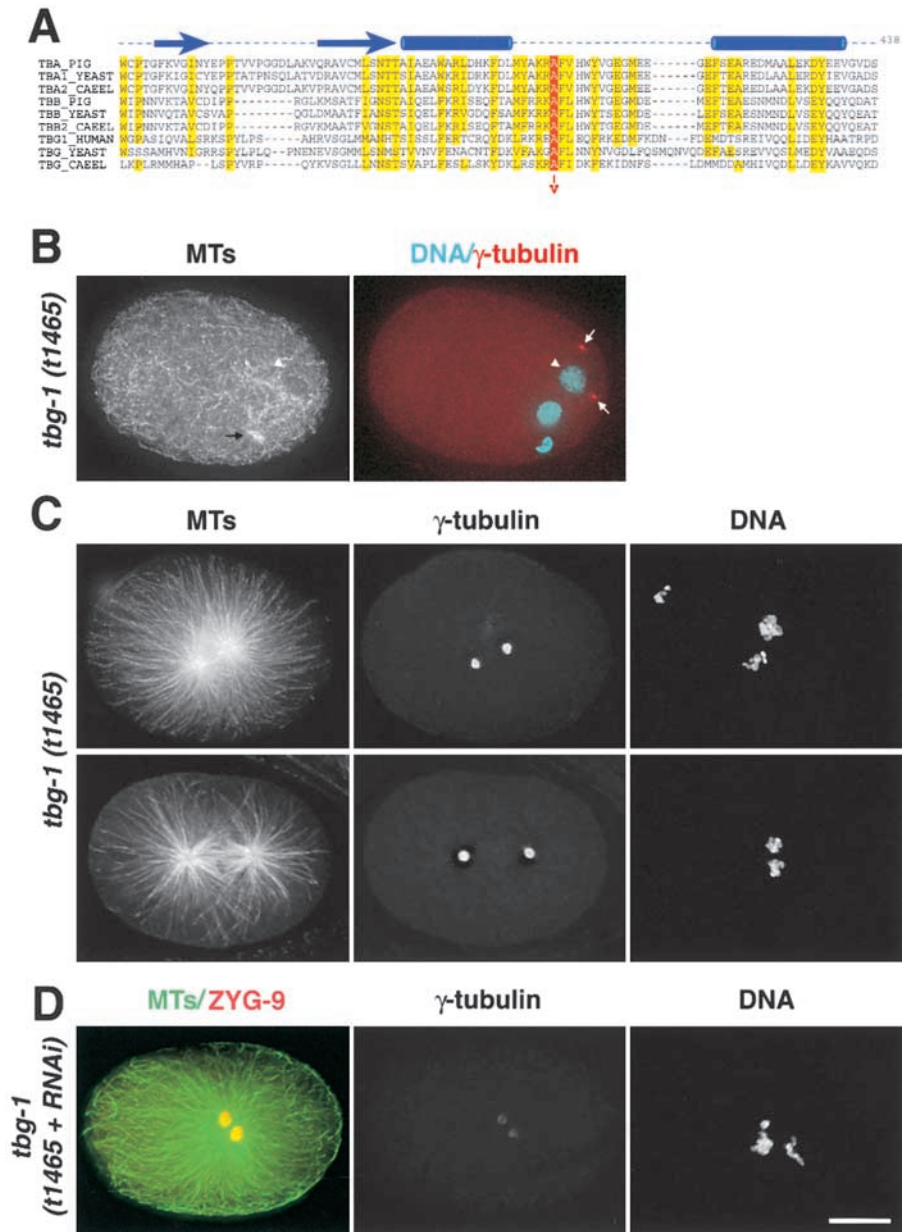

Injection of dsRNA into hermaphrodites inhibits expression of the homologous gene, however preexisting protein remains in the syncytial gonad. Continued production of embryos, which bud off the gonad tip, progressively clears the gonad cytoplasm (which is packaged into the oocytes) over the 24–36 h after injection. To quantitate the extent of γ-tubulin depletion in *tbg-1(RNAi)* embryos, we first performed Western blots on embryos isolated from hermaphrodites 36 h after injection of dsRNA, the time when we normally dissect the worms to obtain one cell stage embryos for analysis (Fig. 2 A). Whereas α-tubulin levels were unaltered by RNAi of *tbg-1,* the amount of γ-tubulin was significantly reduced (to <10% of wild-type levels). The embryo isolation procedure results in a mixed embryo population of all developmental stages, including older embryos that were fertilized much earlier and are therefore less depleted. Thus, 10% is likely a significant overestimate of the amount of γ-tubulin remaining in newly fertilized embryos.

As it is not technically feasible to measure γ-tubulin levels in recently fertilized embryos using Western blotting (there are only 1–2 such embryos per injected worm), we used immunofluorescence to quantify the amount of γ-tubulin remaining at centrosomes in one cell stage *tbg-1(RNAi)* embryos. Antibodies to γ-tubulin and a second centrosomal protein, ZYG-9, were directly labeled with fluorescent dyes and used to stain wild-type and *tbg-1(RNAi)* embryos in parallel. 3D data stacks were collected and deconvolved. ZYG-9 staining was used to circle the 3D volume of the centrosome, and total γ-tubulin and ZYG-9 fluorescence was measured in this volume (Fig. 2, B and C). In *tbg-1(RNAi)* embryos, centrosomal γ-tubulin staining was reduced to ∼2% (2.0 ± 0.9%) of wild-type levels. As a specificity control, we stained wild-type embryos with the same antibody mix to which the antigenic γ-tubulin peptide was added 30 min before use. We found that centrosomal γ-tubulin staining was reduced to ∼1% (0.95 ± 0.28%) of wild-type lev-

A

Grip Motif 1


```
HsGCP3     TKTGDPYHRSLVQHILSLVSHPVLSFLYRWIYDGELEDTYHEFFVAS----------DPTVKTDRLWHDKYTLRKKSMIPSFMTMDQSRKVLLIGKSINF
Xlxgrip109 TKTGDPYHMRSLVQHILGLVAYPILNFLYRWIYDGELEDTYHEFFVAS----------DPVVKTDRLWHDKYSLRKSMIPSFMTMDQSRKVLLIGKSINF
DmDgrip91  LDNGNDMVNKLVEDFLTAICCPLVRMISKWIIEGGISDMHREFFVKS----------IKDVGVDRLWHDKFRLRLPMLPKFVPMDMANKIFMTGKSINF
SpAlp6     NVHGDPLIQELSDKILTEITGPLYEMIENWIIKGGISDVPDPYQEFFVKEKNGSE----SHDHGGQGDVVWKGKRYTLRDKELIPKFSEELVDKIFLIGKSLNF
CaT18252   TNHGDPIKRGIAVTAFTEVVKPYYNIVEHHIVKGELIDNNNEFFIIFDQEQNE----------FNSIKLLPKKIPAFIKS--SDKIFQIGKTLIF
ScSpc98    KSHGDLTIRKIATNLFNSMISLYYEIMNWLTKGLLRATVYGKYFIAEN----------TDTHGTDDDFIYHIPIEFWQGKYIFNFEIKLAYKIFNIGKSVIF
CeGrip-1   SFDSDQ--KSLLDVILDYTLGVFCNQMHERVNTTQEIPTS-DKNIIEKNEQSG----------ELFLRKIPIFITDSDARILLEIGKSLPH
CeGrip-2   VFSAGNV--VQNLDDVF-QAGWKVFARSIGRLVCKFEADHMDYFIRVWSTKQMTDSQCKTLVPSNPSRQIKSSRYVVIESLCPDFFKK-YLDILVRCAEFGDS
             G    L   LL         L  WI G   L      HEF I                               L   PF      IL GK
```

Grip Motif 2


```
HsGCP3     LDVLNKKYSLLDHMQAMRRYLLLGQ-GDFIRHLMDL-LKPE-LVRPATTLYQHNLTGILETAVRATNAQFDSP-------EILRRLDVRLLEVSP------
Xlxgrip109 LDVLNKNYNLLEHMQAMRRYLLLGQ-GDFIRHLMDL-LKPE-LVRPATTLYQHNLTGILETAVRATNAQFDNP-------EILKRLDVRLLEVSP------
DmDgrip91  LDIMVGPHKLLDHLHGHMRYLLLGQ-GDFISILIEN-MKNE-LERPADIYANDLTSMLDSALRCTNAQYDDP-------DILNRLDVIVQRPFN------
SpAlp6     VYLMEEVFHLTDHLKAIRKYLLLGQ-GDFVDLLNES-LGNS-LDQPANTFRHNLTASLESAIRSSNASYEPEY-------VLKRDARLLELSH------
CaT18252   TQIIQGNNKLFTHVYNFKRFYFMET-NDFIDAIMVK-GKDV-FNESSVNISSTYLRKVLQDAIQISSVKNFEY-------VDRLDSRVLNPQH------
ScSpc98    NQILNQKFHYRDVVFALKNILLMGK-SDFMDALIEK-ANDI-LATPSDSLPNYKLTRVLQEAVQLSSLRHLMNSPRN--SSVINGLDARVLDLGH------
CeGrip-1   MRMVMETGRLKEHVLKSTSFFFLSD-PRFTTTLYTI-IKEA--SQGLRVGSTTLSRQTVSSALAAALESCQSTQNISDKEKKVKKLMFTLDALTSTG----
CeGrip-2   ACLLREITSATNVDQAIHDIHDLLIKGSCAHDVMLFGLKADILQKPIDEVGNIRRKKLTHDVLGAAAEKHHPFWKYFSF--VIDKQNVFEMLGQRTSLGGN
              L      L   LR FLL   GF L            P            L            L  L      LLL
```

```
HsGCP3     ----GDTGWDVFSLDYHVD-GPIATVFTRECMS-----HYLRVFNFLWRAKRMEYIILTD-IRKGHMCNAKLLRHMP-----EFSGVLHQCHILASEMVHF
Xlxgrip109 ----GDTGWDVFSLDYHVD-GPIATVFTRECMS-----HYLRVFNFLWRAKRMEYIILTD-IWKGHMCNAKLLKGMP-----ELSGVLHQCHILASEMVHF
DmDgrip91  ----GDIGWNIISLQYIVH-GPLAAMLESTMP------TYKVLFLFLWRMKHMEFVLSMKIWKEQMCNAKALRTMKS-----EIGKASHRLRLFTSEIMHF
SpAlp6     ----GETGWDVFTLEYHVD-SPINVIITPYCSR-----QYLKIFNFLHRLKRIEFALAHSWARVNLGERNVFRNLD------YTKFEWHFVSCHLAEMIHF
CaT18252   ----GNLGWESFTIEYKIDDLPMSYLFEGHQHL-----QYLKHFHFLWLRQLNNLLNWNHFEMFNELNHHVVTKLSS-RNRRPLAKSLSIITSIRFHFTQF
ScSpc98    ----GSVGWDVFTLDYIILY-PPLSLVLNVNRPFGRK--EYLRIFNFLWRFKKNNYFYQKEMLKSNDIIRSFKKIRGYNPLIRDINKLSRISILRTQFQQF
CeGrip-1   -STPNVSSRHQFVQPLRPRYAPQMDLMKPIFSACDD--AYESIFHVIWSIDLARCSTQDASSQNLP-----------------EIQRFLIKNYSLRENATCL
CeGrip-2   NADNLRDNVTPMLFECISVKHDCPIEIEPIISMKAVFILTPVFR--IWIQLHVASYTIANYRDSIRGQMPRSSLGGIDIAMKKHLMHALDAEISSIKQKWVQ
              W F LTV  PL  L           T  LF   W       L L        L  W         LR H
```

```
HsGCP3     IHQHQYYITFEVLECSWDELWNKVQQ---AQDLDHIIAAHVFLDTIISRCLL
Xlxgrip109 IHQHQYYITFEVLECSWDELWNKVLK---AQDLDHIIAAHDVFLDTIISRCLL
DmDgrip91  IHQHQYYVLFEVICCNWVELQKKMQK--ATTLDEILEAHEKFLQTILVGCFV
SpAlp6     VCQLQYYILFEVIISWQELQLAHEKP-NATLDTYIEAHEKYVTSITHKGLL
CaT18252   LNELIAYLSYDVIERENFQQHIVRKLFYNKNQDLLLKSPMNLSEIDPNNDL
ScSpc98    NSKNESYYLNCIIENIRKKFQM-TENKSQHQFDLIRLHNGIKILNGIL
CeGrip-1   LNHLAHVFSIINSTLRKVRCHVSVQL--------ARFLARFLAAIDEKCVD
CeGrip-2   VDLLINLYYERIQKAASLDEYTECQDILASDVTNHMGISELSQLENIKDILN
              Q YL   LEW L  L        DI H   FL  L
```

B

Wild-type | gip-1 (RNAi)

-288s | -350s

-130s | -137s

+114s | +80s

C

Wild-type | gip-1 (RNAi)

MTs/DNA

γ-tubulin

CeGrip-1

Figure 4. **Depletion of CeGrip-1 blocks recruitment of centrosomal γ-tubulin.** (A) CeGrip-1 contains the two grip motifs found in proteins that form complexes with γ-tubulin (Gunawardane et al., 2000). By performing further BLAST searches using the grip motifs as a query sequence, we recently identified a second predicted *C. elegans* protein, CeGrip-2 (C45G3.3), that contains the grip motifs. Here, grip motifs 1 and 2 from CeGrip-1 and CeGrip-2 are aligned with the grip motifs from other proteins homologous to Dgrip91/Spc98p. Amino acids conserved in 80–100% of the sequences are highlighted in yellow. The conserved amino acids that define grip motifs 1 and 2 (Gunawardane et al., 2000) are shown beneath the alignments in red and green, respectively. (B) Panels summarizing a time-lapse sequence of a wild-type (left) and a *gip-1(RNAi)* embryo (right) expressing both GFP–histone and GFP–γ-tubulin. In *gip-1(RNAi)* embryos, the γ-tubulin signal was greatly reduced or, as in this case, absent (see Videos 1 and 2 located at http://www.jcb.org/cgi/content/full/jcb.200202047/DC1). (C) Mitotic wild-type and *gip-1(RNAi)* embryos stained for MTs and DNA (green and red, top), γ-tubulin (middle), and CeGrip (bottom) are shown. CeGrip-1 and γ-tubulin colocalize at centrosomes. Depletion of CeGrip-1 prevents γ-tubulin recruitment to centrosomes and results in an MT phenotype essentially identical to that observed in *tbg-1(RNAi)* embryos. Depletion of CeGrip-2 also results in an MT phenotype essentially identical to that in *tbg-1(RNAi)* embryos (unpublished data). Bars, 10 μm.
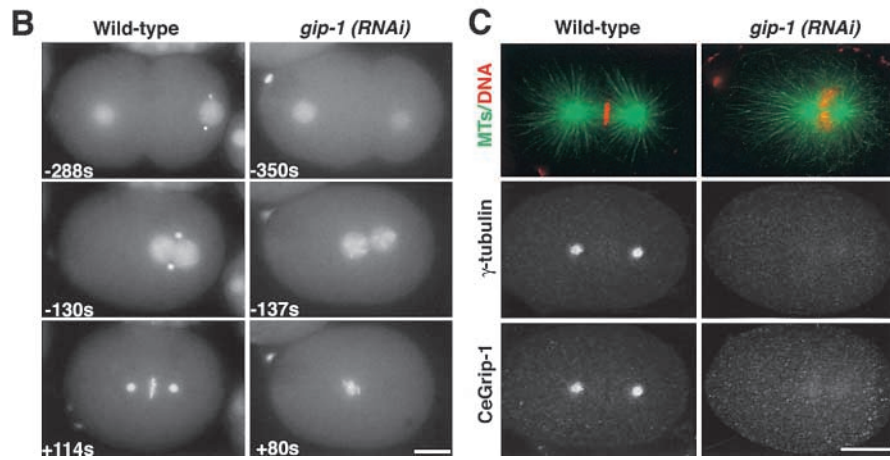
els, confirming the specificity of the centrosomal staining. Thus, relatively robust centrosomal asters can assemble in mitotic embryos in which centrosomal γ-tubulin has been reduced to <2% of wild-type levels.

γ-Tubulin is required to recruit wild-type amounts of centrosomal ZYG-9

Interestingly, centrosomal ZYG-9 was significantly reduced in *tbg-1(RNAi)* embryos (Fig. 2, B and C), to ~30% (31.6 ± 17.0%) of wild-type levels ($P < 0.0001$, *t* test). In the converse experiment, normal levels of γ-tubulin staining were observed in embryos that lack detectable ZYG-9 (embryos obtained from homozygous *zyg-9[it3]* hermaphrodites; unpublished data). These results suggest that γ-tubulin is required to assemble centrosomes that can recruit wild-type amounts of ZYG-9. ZYG-9 remains localized at centrosomes in which the MTs have been depolymerized by nocodazole treatment (Matthews et al., 1998; Fig. 2 D), suggesting that the reduction of ZYG-9 staining in *tbg-1(RNAi)* embryos is not due to a reduction in the number of centrosomally organized MTs. Because of a lack of additional PCM markers in *C. elegans*, we cannot be sure if the defect in ZYG-9 recruitment is specific or the

result of a more general effect of γ-tubulin depletion on the structure of the PCM.

## A point mutation in *tbg-1* results in a phenotype similar to RNAi of *tbg-1*

Because embryos normally stockpile proteins required for cell division, we wanted to use independent means to confirm the assembly of mitotic asters in the absence of functional centrosomal γ-tubulin. To do this, we identified a maternal effect lethal mutation in γ-tubulin. We found that a locus important for spindle assembly, *sas-3* (Gönczy et al., 1999b), mapped in the vicinity of *tbg-1*. *sas-3(t1465)* is a maternal effect mutation; homozygous individuals develop to adulthood because of maternally supplied protein, but these hermaphrodites lay eggs that fail to develop. We rescued the *sas-3(t1465)* defect by injecting F58A4 cosmid DNA, which contains *tbg-1*, into *sas-3* heterozygotes (for details see Materials and methods). Consistent with the rescue results, sequencing of four independent PCRs of the *tbg-1* gene from *sas-3(t1465)* revealed a point mutation (alanine 401 to valine) in *tbg-1*. Although this is a subtle amino acid change, alignment of α-, β-, and γ-tubulin sequences from different species revealed absolute conservation of alanine

401 among tubulins (Fig. 3 A). Structural data implicate the adjacent phenylalanine in the longitudinal contact between tubulin monomers (Nogales et al., 1999), suggesting that this mutation would disrupt head-to-tail interactions between γ-tubulins or between γ-tubulin and αβ-tubulin heterodimers. Based on these results, we refer to the *sas-3(t1465)* mutation as *tbg-1(t1465)*.

To characterize the *tbg-1(t1465)* phenotype, we fixed and stained embryos to visualize DNA, MTs, and γ-tubulin (Fig. 3, B and C). Interestingly, our antibody detected normal levels of γ-tubulin at centrosomes in both interphase (Fig. 3 B) and mitotic (Fig. 3 C) *tbg-1(t1465)* embryos, suggesting that the *t1465* point mutation interferes with the activity of γ-tubulin but not its folding or centrosomal targeting. The MT defects in interphase *tbg-1(t1465)* and *tbg-1(RNAi)* embryos were indistinguishable (compare Fig. 3 B with Fig. 1 A). Interphase centrosomes in *tbg-1(t1465)* embryos failed to assemble MT asters and did not associate with the sperm pronucleus. The mitotic phenotype was similar, but not identical, for the two perturbations. Although mitotic asters were observed and functional spindles failed to assemble, the two centrosomes often separated to a greater extent in *tbg-1(t1465)* embryos than in *tbg-1(RNAi)* embryos (compare Fig. 3 C with Fig. 1 C). In some cases, this resulted in the formation of partial spindle-like structures (Fig. 3 C, bottom). However, the chromosomes on these spindles never congressed to form a metaphase plate; instead they exhibited an alignment defect similar to that seen in the absence of kinetochore function (Oegema et al., 2001). By performing RNAi of *tbg-1* in the *tbg-1(t1465)* mutant, we obtained embryos in which the level of mutant γ-tubulin at centrosomes was reduced to between 5 and 8% of normal *tbg-1(t1465)* levels. We will refer to these as *tbg-1(t1465+RNAi)* embryos. The lower efficiency of RNAi in the mutant is likely because of a reduction in the rate at which the maternal cytoplasm in the gonad is cleared by embryo production. Centrosomes in *tbg-1(t1465+RNAi)* embryos still organized mitotic asters (Fig. 3 D), supporting the conclusion that mitotic centrosomal asters can assemble in the absence of functional γ-tubulin.

Depleting the γ-tubulin–associated protein CeGrip-1 blocks γ-tubulin recruitment and results in the same phenotype as RNAi of *tbg-1*

In all systems where it has been examined, γ-tubulin exists in a heteromeric complex with two members of the Spc97p/Spc98p family of proteins. We used PSI-BLAST to identify H04J21.3 as a possible homologue of the Dgrip91/Spc98p subfamily in *C. elegans*. We sequenced the corresponding cDNA, yk558c5. Because there was no in-frame stop codon upstream of the first ATG, we used RT-PCR with the trans-spliced SL-2 leader to obtain a full-length sequence (available from GenBank/EMBL/DDBJ under accession no. AY099352). This sequence was longer than predicted in WormBase, including three additional NH$_2$-terminal exons from the adjacent cosmid. Consistent with the nomenclature proposed for γ-tubulin–associated proteins in *Drosophila* and *Xenopus* (Zheng et al., 1995; Oegema et al., 1999), we refer to this gene as *gip-1* (for gamma tubulin interacting protein) and the cor-
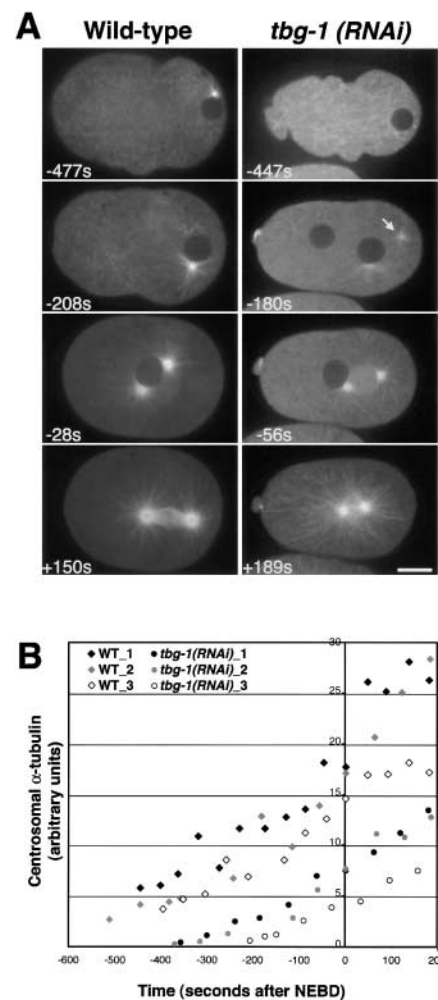
Figure 5. **During mitosis in *tbg-1(RNAi)* embryos, centrosomal α-tubulin fluorescence reaches ~40% of wild-type levels.** (A) Panels summarizing movies of wild-type (left) and *tbg-1(RNAi)* embryos (right), expressing GFP–α-tubulin. Times are with respect to NEBD. See also Videos 3 and 4 located at http://www.jcb.org/cgi/content/full/jcb.200202047/DC1. In wild type, asters are visible at an early stage (−477 s). The asters grow in size (all panels) and become the poles of the mitotic spindle (+150 s). (−447 s) In *tbg-1(RNAi)* embryos there are no detectable asters at early time points. (−180 s) Coincident with the onset of mitotic prophase in wild-type (judged by comparison of GFP–α-tubulin and GFP–histone sequences), centrosomal asters form in the *tbg-1(RNAi)* embryos. At this time, centrosomes (arrow) are often observed to "fly in" to meet the paternal pronucleus. (+189 s) After NEBD, robust mitotic asters form but no spindle assembles. Bar, 10 μm. (B) Kinetic traces of centrosomal α-tubulin fluorescence. Centrosomal fluorescence was quantitated in five wild-type and four *tbg-1(RNAi)* embryos. Three traces are shown for each.

responding protein as CeGrip-1. CeGrip-1 contains both gamma ring protein (grip) motifs (Gunawardane et al., 2000) found in proteins that form complexes with γ-tubulin (Fig. 4 A). In phylogenetic trees, CeGrip-1 groups with the Dgrip91/Spc98p subfamily of grip motif–containing proteins (see phylogenetic tree in online supplemental material located at http://www.jcb.org/cgi/content/full/jcb.200202047/DC1).

To determine if CeGrip-1 is required to recruit γ-tubulin to centrosomes, we used a previously established live assay
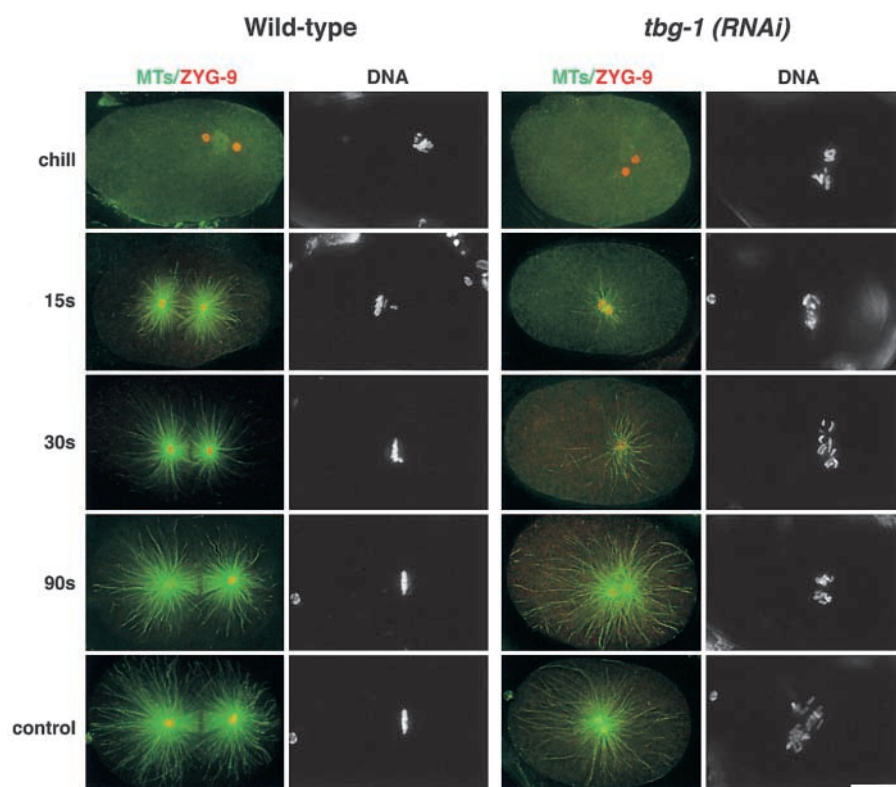
Figure 6. **γ-Tubulin is the kinetically dominant centrosomal MT nucleator.** Embryos were chilled to depolymerize MTs, rewarmed for the indicated amounts of time, and then fixed and stained to visualize MTs and ZYG-9 (green and red, left in each pair), γ-tubulin (unpublished data), and DNA (right in each pair). Control slides that were not chilled were prepared in parallel (control). After chilling, no MTs are seen emanating from centrosomes in either wild-type or *tbg-1(RNAi)* embryos (both MT/ZYG-9 and DNA images are projections of entire data stacks). After 15 s regrowth, numerous short MTs emanate from the centrosomes in wild-type embryos, but in *tbg-1(RNAi)* embryos, only a few centrosomal MTs are observed (these and all subsequent MT/ZYG-9 images are single focal planes). After 30 s regrowth, spindles are found in wild-type embryos (left) and the number and length of MTs have increased in *tbg-1(RNAi)* embryos (right). After 90 s regrowth, the asters in the *tbg-1(RNAi)* embryos (right) are similar to asters in unchilled control *tbg-1 (RNAi)* embryos (bottom right). Bar, 10 μm.

for γ-tubulin recruitment (Hannak et al., 2001). We filmed embryos expressing both GFP–histone and GFP–γ-tubulin. In wild-type embryos, GFP–γ-tubulin localizes to centrosomes during interphase and the amount of centrosomal γ-tubulin increases approximately sixfold as embryos enter mitosis (Fig. 4 B; Hannak et al., 2001). In *gip-1(RNAi)* embryos (*n* = 20), GFP–γ-tubulin was either greatly reduced or absent (Fig. 4 B). To ensure that this was also true for endogenous γ-tubulin, we fixed *gip-1(RNAi)* embryos and stained them for DNA, MTs, γ-tubulin, and CeGrip-1. In wild-type embryos, CeGrip-1 colocalizes with γ-tubulin at centrosomes during interphase (unpublished data) and mitosis (Fig. 4 C, left). In *gip-1(RNAi)* embryos, γ-tubulin fails to target to centrosomes (*n* = 10 embryos; Fig. 4 C, right), consistent with observations in other organisms (Martin et al., 1998; Barbosa et al., 2000; Vardy and Toda, 2000). Consistent with the interdependence of these two proteins during centrosomal recruitment, *tbg-1(RNAi)* embryos also failed to recruit CeGrip-1 to centrosomes (*n* = 5; unpublished data). Depletion of CeGrip-1 (Fig. 4 C) resulted in an MT phenotype essentially identical to that observed in *tbg-1(RNAi)* embryos.

In summary, we have analyzed embryos in which γ-tubulin function was perturbed in four ways: by depletion of γ-tubulin using RNAi; via an alanine 401 to valine maternal effect point mutation in *tbg-1*; by using RNAi to decrease the level of alanine 401 to valine mutant γ-tubulin; and by preventing the assembly of γ-tubulin at centrosomes via depletion of CeGrip-1. In all four cases, the phenotype was essentially the same. During interphase, cytoplasmic MTs were not affected, but assembly of centrosomal asters failed. Centrosomal asters formed as embryos entered mitosis, but spindle assembly never occurred.

During mitosis in *tbg-1(RNAi)* embryos, centrosomal α-tubulin fluorescence reaches ~40% of wild-type levels

Cumulatively, our γ-tubulin perturbation data provide strong evidence that mitotic centrosomal asters assemble in embryos in which γ-tubulin function has been severely compromised. These observations raise a number of important mechanistic questions. First, although mitotic asters ultimately form, how do the kinetics of aster assembly in the γ-tubulin–depleted embryos compare with wild type? To address this issue, we used spinning disk confocal microscopy to analyze *tbg-1(RNAi)* embryos expressing GFP–α-tubulin (Fig. 5 A). Centrosomal α-tubulin fluorescence was quantified for each time point to estimate the number of centrosomally organized MTs (Fig. 5 B). In wild type, astral MTs emanate from the two interphase centrosomes associated with the sperm pronucleus (Fig. 5 A, −477 s). As embryos enter mitosis, centrosomal α-tubulin intensity increases approximately three- to fivefold (Fig. 5, A and B), coincident with a similar fold increase in the amount of centrosomal γ-tubulin (Hannak et al., 2001).

Consistent with our results in fixed embryos, asters were not associated with the sperm pronucleus in early *tbg-1(RNAi)* embryos (Fig. 5 A, −447 s). Between 3 and 5 min before NEBD, which corresponds to mitotic prophase in wild-type embryos, asters became visible and began to increase in size. In some recordings, we were able to watch the centrosomes as they began to nucleate MTs. Initially, these centrosomes were not associated with the sperm pronucleus, but were instead found close to the cortex. As they began to nucleate MTs, the centrosomes rapidly moved toward the sperm pronucleus (Fig. 5 A, −180 s, arrow). Over the time

Figure 7. **Aster formation in γ-tubulin depleted does not require cytoplasmic dynein or ZYG-9.** (A) Wild-type, *dhc-1(RNAi)*, and *dhc-1(RNAi)+ tbg-1(RNAi)* embryos were stained for MTs, DNA, dynein, and γ-tubulin. In wild type (top), dynein (DHC-1) is found in the cytoplasm and enriched around the chromosomes. Depletion of DHC-1 by RNAi (middle) prevents pronuclear migration, centrosome separation, and spindle assembly. Two centrosomal asters form near the posterior cortex of the embryo. Simultaneous depletion of both γ-tubulin and dynein (bottom) results in a qualitatively similar phenotype to dynein depletion alone. (B) Wild-type and *tbg-1(RNAi)+zyg-9(RNAi)* embryos were stained for MTs, DNA, γ-tubulin, and ZYG-9. In embryos depleted of both γ-tubulin and ZYG-9 (bottom), robust mitotic asters are formed. Bar, 10 μm.
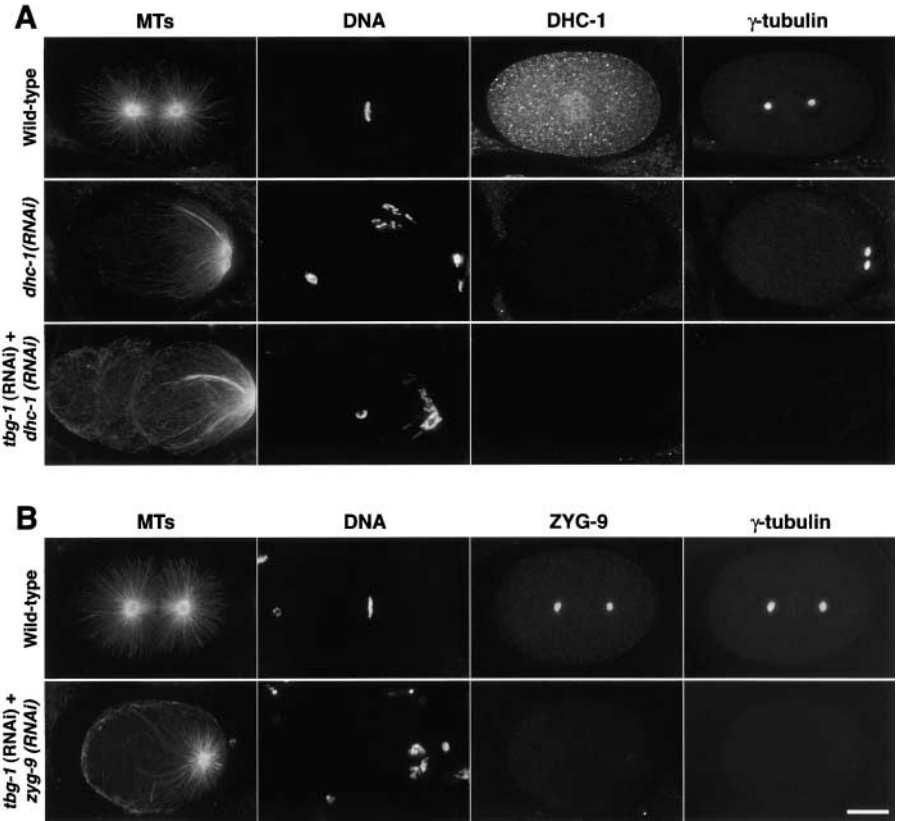
interval beginning 200 s before NEBD, centrosomal α-tubulin fluorescence in *tbg-1(RNAi)* embryos increased in a uniform fashion, reaching ∼40% of wild-type levels by anaphase onset. We interpret this to mean that the asters formed in the absence of γ-tubulin have fewer MTs. These results suggest that although mitotic asters assemble in embryos in which centrosomal γ-tubulin accumulates to only ∼2% of wild-type levels, γ-tubulin is required to achieve a wild-type number of astral MTs.

γ-Tubulin is the kinetically dominant centrosomal MT nucleator

A second important mechanistic question is how do the kinetics of centrosomal MT nucleation in *tbg-1(RNAi)* embryos compare with wild type? Is there evidence for a robust γ-tubulin–independent mechanism for the nucleation of centrosomal MTs? This question is impossible to address from static images of the MT cytoskeleton or even from live kinetic analysis of aster assembly in γ-tubulin–depleted embryos. This is because assembly of mitotic asters (centrosome maturation) occurs over a relatively long period of time (∼400 s) in both wild-type and γ-tubulin embryos, and is a complex phenomenon that includes accumulation of additional PCM and cell cycle–dependent changes in MT dynamics. Therefore, to selectively assay centrosomal nucleation from γ-tubulin–deficient centrosomes, we performed a series of chill and rewarm experiments to examine the kinetics of MT regrowth from centrosomes at short time points. We depolymerized MTs by mounting either wild-type or *tbg-1(RNAi)* embryos on a slide in a thin layer of liquid and incubating them on an aluminum block in an

ice bath for 5 min. The slides were transferred to an aluminum block held at room temperature (22°C–25°C in four experiments) and MTs were allowed to regrow for 0 (chill), 15, 30, or 90 s. The slides were then plunged into liquid nitrogen, fixed, and stained to visualize MTs, DNA, ZYG-9 (Fig. 6), and γ-tubulin (unpublished data). In wild-type embryos, explosive regrowth was observed by 15 s after transfer to room temperature. Although shorter, the number of MTs emanating from centrosomes appeared comparable to that in untreated embryos. After 30 s of regrowth, the MTs formed almost normal-looking spindles with astral MTs that reached out to the cortex. In *tbg-1(RNAi)* embryos rewarmed for 15 s, explosive regrowth was not observed. Instead, only a few short MTs extended from the centrosomes. After 30 s of regrowth, the number and length of MTs in γ-tubulin–depleted embryos had increased, and by 90 s, asters that appeared similar to those in unchilled *tbg-1(RNAi)* control embryos were observed. From these results, we conclude that γ-tubulin is the kinetically dominant centrosomal MT nucleator. Nevertheless, slow nucleation by an uncharacterized mechanism can support partial assembly of mitotic centrosomal asters.

The assembly of γ-tubulin–independent mitotic asters does not require cytoplasmic dynein or ZYG-9

An important remaining question is once nucleated, how are the MTs in *tbg-1(RNAi)* embryos anchored to assemble centrosomal asters? One attractive possibility is that MTs, nucleated either at centrosomes or in the cytoplasm, are organized into centrosomal asters by the activity of cytoplasmic dynein. In cell-free extracts, cytoplasmic dynein is required to assem-

ble mitotic asters in the absence of centrosomes (Verde et al., 1991; Gaglio et al., 1997). To test whether cytoplasmic dynein contributes to the assembly of mitotic asters in *tbg-1(RNAi)* embryos, we performed a double RNAi experiment. In embryos in which cytoplasmic dynein (DHC-1) alone is depleted by RNAi, pronuclear migration fails; the centrosomes do not separate and no recognizable spindle assembles (Gönczy et al., 1999a). However, the centrosomes nucleate two prominent asters that remain positioned in the posterior of the embryo (Fig. 7 A, middle). In embryos depleted of both γ-tubulin and DHC-1 ($n = 10$), centrosomal γ-tubulin was reduced to ~2% (1.9 ± 1.5%) and the amount of cytoplasmic DHC-1 signal to ~11% (11.1 ± 6.5%) of wild-type levels. We interpret this to mean that we have likely depleted at least 90% of the DHC-1, because we cannot assess whether the remaining signal is due to residual DHC-1 or to other cross-reacting cytoplasmic proteins. In the double RNAi embryos, prominent mitotic asters formed. As was the case in the embryos depleted of dynein alone, pronuclear migration failed in *tbg-1(RNAi)+dhc-1(RNAi)* embryos, and the mitotic asters remained associated with the posterior cortex (Fig. 7 A, bottom).

A second candidate for a molecule that could organize mitotic asters in the absence of γ-tubulin is ZYG-9, the *C. elegans* homologue of the XMAP-215/ch-TOG family of MT-associated proteins (Matthews et al., 1998). In *Drosophila* embryos, overexpression of a protein that interacts with mini-spindles (Msps), the *Drosophila* XMAP-215/ch-TOG family member, results in the formation of ectopic asters. Mini-spindles (Msps) localizes to the center of these asters, but γ-tubulin is not present (Lee et al., 2001). To test if XMAP-215/ch-TOG contributes to the assembly of mitotic asters in *tbg-1(RNAi)* embryos, we performed a double RNAi experiment (Fig. 7 B). In *tbg-1(RNAi)+zyg-9(RNAi)* embryos ($n = 10$), centrosomal γ-tubulin was depleted to ~1% (0.82 ± 0.82%) and centrosomal ZYG-9 to ~5% (5.1 ± 3.9%) of wild-type levels, but robust mitotic asters still formed. Thus, neither cytoplasmic dynein nor ZYG-9 contribute to the assembly of γ-tubulin–independent mitotic asters in *C. elegans*.

Discussion

During interphase, γ-tubulin is required to assemble centrosomal asters but is not required to nucleate or stabilize cytoplasmic MTs

Our results indicate that γ-tubulin is required to assemble centrosomal asters during interphase. Consistent with our analysis in *C. elegans*, injection of γ-tubulin antibodies into vertebrate tissue culture cells during interphase blocked the regrowth of centrosomal MTs after cold treatment (Joshi et al., 1992). The failure of interphase aster formation in the absence of γ-tubulin is also consistent with data from *spd-2 (oj29ts)* mutant embryos. This locus has not been cloned, but mutant embryos fail to recruit γ-tubulin to centrosomes and fail to form interphase asters (O'Connell et al., 2000). Interestingly, in the absence of associated MTs, interphase centrosomes fail to associate with nuclei. Concomitant with the onset of aster formation, as the embryos enter mitosis, the centrosomes move rapidly toward the sperm pronucleus and attach to it. The mechanisms that underlie the interaction between centrosomes and nuclei are not well understood (for review see Reinsch and Gönczy, 1998), but our results suggest that in *C. elegans* embryos, MTs are required to establish this interaction. Interestingly, although aster assembly is blocked, inhibition of γ-tubulin function does not affect the numerous cytoplasmic MTs that fill interphase embryos (Fig. 1 A and Fig. 3 B). This suggests that cytoplasmic MTs, the majority of the MTs present in interphase embryos, do not require γ-tubulin for their nucleation or stabilization. The identification of factors that modulate the dynamics of these MTs will be an interesting direction for future studies.

Mitotic centrosomal asters assemble in embryos in which γ-tubulin function is severely compromised

As embryos enter mitosis, centrosomes normally undergo a maturation process characterized by accumulation of additional PCM, including γ-tubulin, concomitant with an increase in the number of centrosomally organized MTs. Consistent with the report by Strome et al. (2001) that asters assemble in mitotic *tbg-1(RNAi)* embryos, we observed assembly of mitotic asters in all of our γ-tubulin perturbations. From these results, we conclude that organized centrosomal asters can assemble during mitosis even when γ-tubulin function is severely compromised. This analysis is consistent with two previous studies performed in *Drosophila*. In *Drosophila* larval brains mutant for the zygotic isoform of γ-tubulin, a variety of abnormal mitotic figures were observed, ranging from MTs without any organization to bipolar arrays. In some cases, significant assembly of centrosomal asters occurred in the absence of detectable γ-tubulin (Sunkel et al., 1995). In a more recent study, well-organized centrosomal asters were observed during prophase in *Drosophila* spermatocytes mutant for the somatic isoform of γ-tubulin (Sampaio et al., 2001). In this case, Western blotting revealed that γ-tubulin levels were severely reduced, although a weak γ-tubulin signal could still be detected at centrosomes by immunofluorescence.

γ-Tubulin is the kinetically dominant centrosomal nucleator

The fact that well-organized centrosomal asters assemble during mitosis in embryos in which γ-tubulin function is severely compromised raises some important mechanistic issues. One key question is how are these MTs nucleated? Is the assembly of these mitotic asters evidence for a robust alternative centrosomal nucleator? To address this issue, we examined the kinetics of MT regrowth from mitotic centrosomes after cold-induced depolymerization. We showed that nucleation from γ-tubulin–depleted centrosomes is severely compromised. Nevertheless, over a time frame ~5–10-fold longer than in wild type, the number of centrosomally organized MTs recovers to about half of wild-type levels. From these results we can conclude that γ-tubulin is the kinetically dominant centrosomal MT nucleator. Nevertheless, in embryos in which γ-tubulin function is severely compromised, slow nucleation by an uncharacterized mechanism can support assembly of mitotic centrosomal asters. Although we

don't know what this uncharacterized mechanism is, there are several formal possibilities. One possibility, which we think is unlikely (see below), is that MTs spontaneously nucleated in the cytoplasm are subsequently reorganized to form asters. A second possibility that we cannot completely exclude is that a very low level of residual γ-tubulin function is sufficient to account for the slow rate of centrosomal nucleation that we observe. A final possibility is that there is an alternative weak nucleator present at centrosomes.

Assembly of centrosomal asters in γ-tubulin–depleted embryos does not require cytoplasmic dynein–mediated self-organization

Because γ-tubulin is also thought to play a role in the anchoring of centrosomal MTs, a second key question is once nucleated, how are the MTs in γ-tubulin–depleted embryos anchored to assemble centrosomal asters? An appealing mechanism is that MTs nucleated in the cytoplasm form a focused centrosomal array due to motor-dependent self-organization similar to that used to organize spindle poles (for review see Wittmann et al., 2001). This seems unlikely for two reasons. First, in our regrowth experiments in *tbg-1(RNAi)* embryos, we did not observe cytoplasmic MTs that appeared to subsequently organize, instead nucleated MTs were centrosomally anchored even at very short time points. Second, we have shown that depleting both γ-tubulin and cytoplasmic dynein (DHC-1) at the same time does not block centrosomal aster formation. In *Xenopus* egg extracts (Verde et al., 1991) and vertebrate somatic cells (Gaglio et al., 1997), mitotic aster self-organization requires dynein function. However, we cannot rule out rapid self-organization involving a different minus-end–directed motor. Uncovering the mechanism that organizes centrosomal asters in γ-tubulin–depleted embryos will be an informative direction for future work. It will also be interesting to determine the extent to which γ-tubulin–independent anchoring mechanisms contribute to the organization of centrosomal MTs in wild-type embryos. One possibility consistent with our data is that the anchoring mechanism that organizes mitotic asters in γ-tubulin–depleted embryos is normally used to anchor astral MTs in wild-type, whereas a γ-tubulin–dependent mechanism is used to stabilize or anchor spindle/kinetochore MTs.

Materials and methods

C. elegans culture and strains
sas-3(t1465) mutant worms were obtained from Ralf and Heinke Schnabel (Max Planck Institut fuer Biochemie, Martinsried, Germany). Wild-type worms were grown at 16°C and *sas-3(t1465)* mutants at 20°C. Strains expressing GFP fusion proteins in the germline were generated and maintained as previously described (Oegema et al., 2001).

Rescue of the *sas-3(t1465)* defect
The *sas-3(t1465)* defect was rescued by coinjecting a mixture of F58A4 cosmid DNA (15 ng/μl), which contains *tbg-1*, with Bluescript (100 ng/μl) and pPD93.97 (*myo-3::GFP*; 20 ng/μl) into both gonads of *sas-3[(t1465)unc-32/qC1 III]* heterozygotes. The plasmid pDP93.97 was obtained from Andy Fire (Carnegie Institute of Washington). Transformed (fluorescent) progeny of the injected worms homozygous for the *sas-3(t1465)* mutation (Unc) were picked to separate plates and tested for the production of viable embryos. 4/60 transformed Uncs produced viable progeny. Of these, 122/434 embryos developed at least to L1 larvae. Untransformed homozygous progeny produced only dead embryos (0/247).

RNAi
For production of dsRNA to *tbg-1* (ctcaagccttctggaaatcg, gcattgcatcgtccat-cata or tcctcgataatgctgcactg, cttttgtacgaccgccttgt), *gip-1* (agaatgagcagagcg-gagag, gcgagctcttttcgatttg), and *zyg-9* (ggaagatgaggaagtggtc, atagcag-catttcggacgtt), the primers in parentheses with tails containing T3 and T7 promoters were used to amplify regions from genomic N2 DNA (*zyg-9*) or the cDNAs yk80h7 or yk496c1 (*tbg-1*) or yk558c5 (*gip-1*). PCR products were transcribed and dsRNA prepared as previously described (Oegema et al., 2001). RNA for *dhc-1* was prepared as described by Gönczy et al. (1999a). RNAs were injected at concentrations between 1 and 4 mg/ml. For the double RNAi experiments, one part *dhc-1* or *zyg-9* RNA was mixed with three parts *tbg-1* RNA before injection.

Time-lapse microscopy and quantification of centrosomal α-tubulin fluorescence
Live analysis and RNAi in strains expressing GFP fusion were performed as previously described (Oegema et al., 2001). Centrosomal GFP–α-tubulin fluorescence was quantified from live recordings made using spinning disc confocal microscopy as described by Hannak et al. (2001). For qualitative analysis of phenotypes, GFP–α-tubulin images were collected every 8 s using 500–1,000-ms exposure at ~40% power on the 50-mW argon laser. To minimize the contribution of photobleaching, confocal GFP–α-tubulin images were acquired every 45–60 s in quantitated sequences.

Antibodies and immunofluorescence
Antibodies to the COOH-terminal peptides of γ-tubulin and CeGrip (Hannak et al., 2001) and antibodies to DHC-1 (Gönczy et al., 1999a) have been previously described; the rabbit anti–ZYG-9 was a gift of A. Pozniakovsky (Max Planck Institute of Molecular Cell Biology and Genetics). For immunofluorescence, antibodies to γ-tubulin and ZYG-9 were directly labeled with Cy3 and Cy5 (Amersham Pharmacia Biotech) as described by Oegema et al. (2001) and were used at a concentration of 1 μg/ml. In multilabel experiments using anti-CeGrip (1 μg/ml) or anti–DHC-1 (1:200), embryos were incubated with goat anti–rabbit-Fab fragments (5 μg/ml; Jackson ImmunoResearch Laboratories) to convert the first rabbit antibody to a "goat" antibody before incubation with the second rabbit antibody. DM1α was used at a dilution of 1:1,000 to visualize MTs. Embryos were fixed and processed for immunofluorescence as previously described (Oegema et al., 2001). Nocodazole treatment to depolymerize MTs was performed as described by Hannak et al. (2001).

MT regrowth experiments
20 hermaphrodites were put into 4 μl of water under a 22 × 22 coverslip on polylysine-coated slides. Gentle pressure was applied to squeeze the embryos out of the hermaphrodites. Slides were placed on an aluminum block in an ice bath under a humidifying cover for 5 min, transferred to an aluminum block held at room temperature (22°C–25°C in four different experiments) for 0, 15, 30 or 90 s, and plunged into liquid nitrogen followed by processing for immunofluorescence as described.

Western blotting of embryos
L4 larvae were injected with *tbg-1* RNA. After 36 h at 20°C, 160 *tbg-1(RNAi)* or control worms were transferred to tubes containing 1 ml of M9 (Lewis and Fleming, 1995). The worms were pelleted by spinning at 200 *g* for 1 min. The wash was repeated two times, leaving the worms in 50 μl of M9. 50 μl of fresh 2× bleach solution (7.5 μl H_2O, 25 μl 2 M NaOH, 17.5 μl bleach) was added and the tube was vortexed for 3 min to dissolve the hermaphrodites. Embryos were pelleted by spinning at 1,000 *g* for 1 min. All of the solution except 10 μl was removed and the embryos were washed by adding 400 μl of 0.1 M Tris, pH 7.5, 100 mM NaCl, 0.1% Tween 20. The wash step was repeated two times, leaving the isolated embryos in 10 μl of buffer. 10 μl of 2× sample buffer was added and the sample was sonicated for 10 min at 80°C in a waterbath sonicator. Samples were heated to 95°C for 5 min and analyzed using SDS-PAGE followed by immunoblotting. Anti–γ-tubulin antibody (1 μg/ml) and the monoclonal anti–α-tubulin antibody (1:1,000; Sigma-Aldrich) were used. Binding of γ-tubulin antibody was detected with an HRP-conjugated secondary antibody (1:3,000; Bio-Rad Laboratories). The same blot was subsequently probed for α-tubulin using an alkaline phosphatase–conjugated secondary antibody (1:2,000; Jackson ImmunoResearch Laboratories).

Quantification of centrosomal fluorescence in fixed images
For quantification of centrosomal fluorescence in fixed images, centrosomes were circled in all planes of each deconvolved 3D image stack. The average fluorescence intensity in this volume and in a similarly sized

background volume were determined using Metamorph software (Universal Imaging Corp.). Integrated centrosomal fluorescence was obtained by subtracting the background value and multiplying by the volume of the centrosomal region. To quantify cytoplasmic dynein fluorescence, the integrated intensity of a fixed volume was determined and nonspecific background fluorescence of an identical volume, produced by the secondary antibody alone, was subtracted.

Online supplemental material

In the supplemental videos for Fig. 4 B (supplemental material located at http://www.jcb.org/cgi/content/full/jcb.200202047/DC1), γ-tubulin accumulation was followed in wild-type (Video 1) and *gip-1(RNAi)* embryos (Video 2) expressing GFP–histone and GFP–γ-tubulin. In the supplemental videos for Fig. 5, the MT cytoskeleton in GFP–α-tubulin–expressing wild-type (Video 3) and *tbg-1(RNAi)* embryos (Video 4) is shown. The oocyte-derived pronucleus is initially on the left and the sperm pronucleus is on the right in all videos. Playback right is 10 frames/second. A phylogenetic tree of grip domain–containing proteins shows that CeGrip-1 groups with the Dgrip91/Spc98p protein subfamily (Fig. S1).

References

Alberts, B., D. Bray, J. Lewis, M. Raff, K. Roberts, and J. Watson. 1994. Molecular Biology of the Cell. Garland Publishing, Inc., New York. 1294 pp.

Barbosa, V., R.R. Yamamoto, D.S. Henderson, and D.M. Glover. 2000. Mutation of a *Drosophila* γ-tubulin ring complex subunit encoded by discs degenerate-4 differentially disrupts centrosomal protein localization. *Genes Dev.* 14: 3126–3139.

Felix, M.A., C. Antony, M. Wright, and B. Maro. 1994. Centrosome assembly in vitro: role of γ-tubulin recruitment in *Xenopus* sperm aster formation. *J. Cell Biol.* 124:19–31.

Frankel, F.R. 1976. Organization and energy-dependent growth of microtubules in cells. *Proc. Natl. Acad. Sci. USA.* 73:2798–2802.

Gaglio, T., M.A. Dionne, and D.A. Compton. 1997. Mitotic spindle poles are organized by structural and motor proteins in addition to centrosomes. *J. Cell Biol.* 138:1055–1066.

Gönczy, P., S. Pichler, M. Kirkham, and A.A. Hyman. 1999a. Cytoplasmic dynein is required for distinct aspects of MTOC positioning, including centrosome separation, in the one cell stage *Caenorhabditis elegans* embryo. *J. Cell Biol.* 147:135–150.

Gönczy, P., H. Schnabel, T. Kaletta, A.D. Amores, T. Hyman, and R. Schnabel. 1999b. Dissection of cell division processes in the one cell stage *Caenorhabditis elegans* embryo by mutational analysis. *J. Cell Biol.* 144:927–946.

Gunawardane, R.N., O.C. Martin, K. Cao, L. Zhang, K. Dej, A. Iwamatsu, and Y. Zheng. 2000. Characterization and reconstitution of *Drosophila* γ-tubulin ring complex subunits. *J. Cell Biol.* 151:1513–1524.

Hannak, E., M. Kirkham, A.A. Hyman, and K. Oegema. 2001. Aurora-A kinase is required for centrosome maturation in *Caenorhabditis elegans*. *J. Cell Biol.* 155:1109–1116.

Jeng, R., and T. Stearns. 1999. γ-Tubulin complexes: size does matter. *Trends Cell Biol.* 9:339–342.

Joshi, H.C., M.J. Palacios, L. McNamara, and D.W. Cleveland. 1992. γ-Tubulin is a centrosomal protein required for cell cycle-dependent microtubule nucleation. *Nature.* 356:80–83.

Kellogg, D.R., M. Moritz, and B.M. Alberts. 1994. The centrosome and cellular organization. *Annu. Rev. Biochem.* 63:639–674.

Keryer, G., H. Ris, and G.G. Borisy. 1984. Centriole distribution during tripolar mitosis in Chinese hamster ovary cells. *J. Cell Biol.* 98:2222–2229.

Lee, M.J., F. Gergely, K. Jeffers, S.Y. Peak-Chew, and J.W. Raff. 2001. Msps/

XMAP215 interacts with the centrosomal protein D-TACC to regulate microtubule behaviour. *Nat. Cell Biol.* 3:643–649.

Lewis, J.A., and J.T. Fleming. 1995. Basic culture methods. *In Caenorhabditis elegans*. Vol. 48. H.F. Epstein and D.C. Shakes, editors. Academic Press, San Diego, CA. 3–29.

Martin, O.C., R.N. Gunawardane, A. Iwamatsu, and Y. Zheng. 1998. Xgrip109: a γ-tubulin–associated protein with an essential role in γ-tubulin ring complex (γTuRC) assembly and centrosome function. *J. Cell Biol.* 141:675–687.

Matthews, L.R., P. Carter, D. Thierry-Mieg, and K. Kemphues. 1998. ZYG-9, a *Caenorhabditis elegans* protein required for microtubule organization and function, is a component of meiotic and mitotic spindle poles. *J. Cell Biol.* 141:1159–1168.

Meads, T., and T.A. Schroer. 1995. Polarity and nucleation of microtubules in polarized epithelial cells. *Cell Motil. Cytoskeleton.* 32:273–288.

Moritz, M., M.B. Braunfeld, J.C. Fung, J.W. Sedat, B.M. Alberts, and D.A. Agard. 1995a. Three-dimensional structural characterization of centrosomes from early *Drosophila* embryos. *J. Cell Biol.* 130:1149–1159.

Moritz, M., M.B. Braunfeld, V. Guenebaut, J. Heuser, and D.A. Agard. 2000. Structure of the γ-tubulin ring complex: a template for microtubule nucleation. *Nat. Cell Biol.* 2:365–370.

Moritz, M., M.B. Braunfeld, J.W. Sedat, B. Alberts, and D.A. Agard. 1995b. Microtubule nucleation by γ-tubulin-containing rings in the centrosome. *Nature.* 378:638–640.

Moritz, M., Y. Zheng, B.M. Alberts, and K. Oegema. 1998. Recruitment of the γ-tubulin ring complex to *Drosophila* salt-stripped centrosome scaffolds. *J. Cell Biol.* 142:775–786.

Nogales, E., S.G. Wolf, and K.H. Downing. 1998. Structure of the α/β tubulin dimer by electron crystallography. *Nature.* 391:199–203.

Nogales, E., M. Whittaker, R.A. Milligan, and K.H. Downing. 1999. High-resolution model of the microtubule. *Cell.* 96:79–88.

O'Connell, K.F., K.N. Maxwell, and J.G. White. 2000. The spd-2 gene is required for polarization of the anteroposterior axis and formation of the sperm asters in the *Caenorhabditis elegans* zygote. *Dev. Biol.* 222:55–70.

Oakley, B.R. 2000. γ-Tubulin. *Curr. Top. Dev. Biol.* 49:27–54.

Oegema, K., C. Wiese, O.C. Martin, R.A. Milligan, A. Iwamatsu, T.J. Mitchison, and Y. Zheng. 1999. Characterization of two related *Drosophila* γ-tubulin complexes that differ in their ability to nucleate microtubules. *J. Cell Biol.* 144:721–733.

Oegema, K., A. Desai, S. Rybina, M. Kirkham, and A.A. Hyman. 2001. Functional analysis of kinetochore assembly in *Caenorhabditis elegans*. *J. Cell Biol.* 153:1209–1226.

Osborn, M., and K. Weber. 1976. Cytoplasmic microtubules in tissue culture cells appear to grow from an organizing structure towards the plasma membrane. *Proc. Natl. Acad. Sci. USA.* 73:867–871.

Pereira, G., and E. Schiebel. 1997. Centrosome-microtubule nucleation. *J. Cell Sci.* 110:295–300.

Reinsch, S., and P. Gönczy. 1998. Mechanisms of nuclear positioning. *J. Cell Sci.* 111:2283–2295.

Sampaio, P., E. Rebollo, H. Varmark, C.E. Sunkel, and C. Gonzalez. 2001. Organized microtubule arrays in γ-tubulin-depleted *Drosophila* spermatocytes. *Curr. Biol.* 11:1788–1793.

Schiebel, E. 2000. γ-Tubulin complexes: binding to the centrosome, regulation and microtubule nucleation. *Curr. Opin. Cell Biol.* 12:113–118.

Schnackenberg, B.J., A. Khodjakov, C.L. Rieder, and R.E. Palazzo. 1998. The disassembly and reassembly of functional centrosomes in vitro. *Proc. Natl. Acad. Sci. USA.* 95:9295–9300.

Stearns, T., and M. Kirschner. 1994. In vitro reconstitution of centrosome assembly and function: the central role of γ-tubulin. *Cell.* 76:623–637.

Strome, S., J. Powers, M. Dunn, K. Reese, C.J. Malone, J. White, G. Seydoux, and W. Saxton. 2001. Spindle dynamics and the role of γ-tubulin in early *Caenorhabditis elegans* embryos. *Mol. Biol. Cell.* 12:1751–1764.

Sunkel, C.E., R. Gomes, P. Sampaio, J. Perdigao, and C. Gonzalez. 1995. γ-Tubulin is required for the structure and function of the microtubule organizing centre in *Drosophila* neuroblasts. *EMBO J.* 14:28–36.

Tassin, A.M., and M. Bornens. 1999. Centrosome structure and microtubule nucleation in animal cells. *Biol. Cell.* 91:343–354.

Vardy, L., and T. Toda. 2000. The fission yeast γ-tubulin complex is required in G(1) phase and is a component of the spindle assembly checkpoint. *EMBO J.* 19:6098–6111.

Verde, F., J.M. Berrez, C. Antony, and E. Karsenti. 1991. Taxol-induced microtubule asters in mitotic extracts of *Xenopus* eggs: requirement for phosphorylated factors and cytoplasmic dynein. *J. Cell Biol.* 112:1177–1187.

Vogel, J.M., T. Stearns, C.L. Rieder, and R.E. Palazzo. 1997. Centrosomes isolated from *Spisula solidissima* oocytes contain rings and an unusual stoichiometric ratio of α/β tubulin. *J. Cell Biol.* 137:193–202.

Wiese, C., and Y. Zheng. 1999. γ-Tubulin complexes and their interaction with microtubule-organizing centers. *Curr. Opin. Struct. Biol.* 9:250–259.

Wiese, C., and Y. Zheng. 2000. A new function for the γ-tubulin ring complex as a microtubule minus-end cap. *Nat. Cell Biol.* 2:358–364.

Wittmann, T., A. Hyman, and A. Desai. 2001. The spindle: a dynamic assembly of microtubules and motors. *Nat. Cell Biol.* 3:E28–E34.

Zheng, Y., M.L. Wong, B. Alberts, and T. Mitchison. 1995. Nucleation of microtubule assembly by a γ-tubulin-containing ring complex. *Nature.* 378:578–583.